

AERI-ER at the SHEBA Ice Station: Far Infrared Water Vapor Continuum Measurements

D. C. Tobin, R. O. Knuteson, H. E. Revercomb, and V. P. Walden
Cooperative Institute for Meteorological Satellite Studies
University of Wisconsin
Madison, Wisconsin

S. A. Clough and E. J. Mlawer
Atmospheric and Environmental Research, Inc.
Cambridge, Massachusetts

R. G. Ellingson
Department of Meteorology
University of Maryland, College Park

Introduction

For an accurate understanding of earth's climate, it is essential to know the spectral absorption properties of water vapor, in addition to how its distribution depends on geographic location and altitude. Clough et al. (1992), Sinha and Harries (1995), and Stamnes et al. (1998) have shown the importance of the transparent portion of the water vapor rotational band from 250 cm^{-1} to 600 cm^{-1} to earth's energy balance. Knowledge of radiative transfer for clear skies in this spectral region is important for the following reasons: 1) For cold, dry conditions frequently encountered at high latitudes, this spectral region becomes more transparent and strongly influences the near surface contribution to the infrared cooling to space. 2) At high altitudes, similar conditions are also encountered and this region therefore plays a significant role in radiative cooling on a global scale. 3) Measurements in this spectral region are useful to theoretical studies of $\text{H}_2\text{O-X}$ collisions and spectral lineshapes. 4) Accurate remote sensing of atmospheric water vapor for both up- and down-looking sensors requires an accurate radiative transfer model near the centers of water vapor ro-vibrational bands.

At high latitudes, it is often dry enough that narrow "microwindows," or regions in between spectral line centers, become transparent in the strong pure rotational band of water vapor. This is illustrated in the top panel of Figure 1, which shows ground-based clear-sky downwelling radiances observed with atmospheric emitted radiance interferometer (AERI) systems at the Atmospheric Radiation Measurement (ARM) Southern Great Plains (SGP) Cloud and Radiation Testbed (CART) site in central Oklahoma on a particularly warm, humid day, and at the Surface Heat

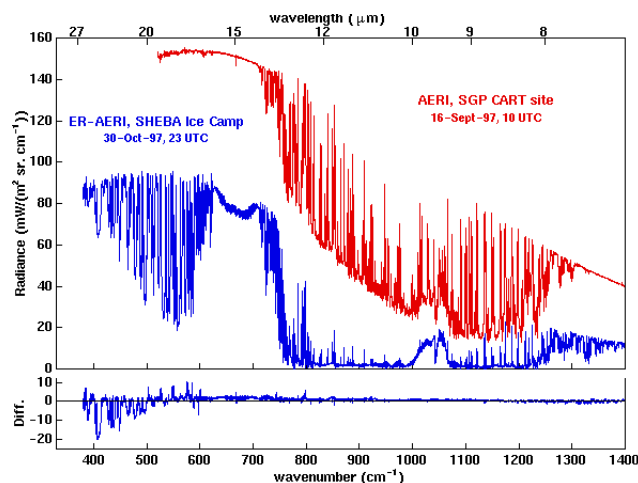


Figure 1. Comparison of clear-sky downwelling radiance spectra measured with the University of Wisconsin AERI system at the SGP CART site near Lamont, Oklahoma, and with the extended range AERI (AERI-ER) at the SHEBA Ice Station, 300 km north of Barrow, Alaska. The bottom panel shows the radiance difference (observed-calculated) between the SHEBA AERI-ER spectrum and a line-by-line calculation done using the CKDv2.2 water vapor continuum model. (For a color version of this figure, please see http://www.arm.gov/docs/documents/technical/conf_9803/tobin-98.pdf).

Budget of the Arctic Ocean (SHEBA) ice station under much cooler and drier conditions. For the SGP CART site case, the precipitable water vapor was $\sim 4.0\text{ cm}$ and the near ground air temperature was $\sim 300\text{ K}$; while for the SHEBA case, these values were $\sim 0.35\text{ cm}$ and $\sim 250\text{ K}$, respectively. The underlying envelope of emission for each case is due

mainly to the far-wings of spectral lines within the pure rotational band of water vapor. For the SGP CART site spectrum, absorption, due to water vapor at $\sim 600\text{ cm}^{-1}$ and longer wavelengths, is large enough such that there is no transmission to space and the detected radiances are equal to the Planck emission at the ambient temperature. For the drier SHEBA case, however, microwindows from $\sim 380\text{ cm}^{-1}$ to 600 cm^{-1} are somewhat transparent, leading to lower observed radiances representative of higher altitudes and colder temperatures. At these lower temperatures, the peak of the Planck Function shifts to longer wavelengths and subsequently the transmission properties of the atmosphere in this spectral region are crucial for climate and energy balance related issues. In particular, others (Clough et al. 1992; Ellingson and Wiscombe 1996; Stamnes et al. 1998) have cited the importance of the water vapor continuum in these issues. Thus, an AERI with extended longwave spectral coverage (AERI-ER) to $\sim 26\text{ }\mu\text{m}$ was deployed to the SHEBA site, in part for the validation and testing of current clear-sky radiance calculations. The bottom panel of Figure 1 shows the radiance difference (observed-calculated) between the SHEBA AERI-ER spectrum and a line-by-line calculation performed using the CKDv2.2 water vapor continuum model. Large differences in the extended longwave region in between water vapor spectral line centers are attributed to errors in the air-broadened water vapor continuum absorption, and are the focus of this paper.

AERI-ER at the SHEBA Ice Station

The AERI-ER extends the longwave cutoff of the useful spectral range of the instrument to longer wavelengths (smaller wavenumbers) than a standard AERI system. This is accomplished by choosing a longwave MCT detector that peaks at longer wavelengths and replaces the optical elements of the interferometer to remove any materials that are optically absorbing in the 400 cm^{-1} to 600 cm^{-1} range. Whereas the noise performance limits the spectral range of the standard AERI to about 525 cm^{-1} , the AERI-ER has similar performance out to 420 cm^{-1} and is useable with time averaging to beyond 400 cm^{-1} . The tradeoff for this enhanced longwave performance is about a 50% degradation of the performance compared to a standard AERI in the 600 cm^{-1} to 1500 cm^{-1} region. The performance in the 1800 cm^{-1} to 3000 cm^{-1} range is the same for both instruments since a separate InSb detector is used in each case. The radiometric calibration accuracy for the AERI-ER is comparable to that of a standard AERI system, i.e., better than 1% of ambient blackbody radiance.

Water Vapor Continuum in the 300 cm^{-1} to 650 cm^{-1} Region

Briefly, in the context of the present work, the water vapor continuum is defined in terms of the “local” lineshape by Clough et al. (1980). (The local absorption coefficient accounts for the cumulative effects of all lines with 25 cm^{-1} of their respective centers using an assumed lineshape.) The continuum is further reduced in terms of its well-known dependence on absorber and broadener densities and is represented by self- and air-broadened continuum coefficients, C_s^0 and C_f^0 , which can vary with wavenumber and temperature. The coefficients represent the cumulative difference over all spectral lines between the total absorption coefficient and the local absorption coefficient. In the earth’s lower atmosphere, continuum absorption in spectral regions near the centers of water vapor bands is generally dominated by air-broadening, while window regions are dominated by self-broadening.

For the $\sim 350\text{ cm}^{-1}$ to 650 cm^{-1} region, laboratory measurements of Burch et al. (1979) at room temperature have formed the basis of a quantitative development of the water vapor continuum. Based on these measurements and others, Clough et al. (1980) used a semi-empirical lineshape formulation, known as CKDv0 (Clough, Kneizys, and Davies, version 0), to account for Burch’s measurements and their deviation from Lorentzian lineshape behavior. In this formulation, C_s^0 is dependent on temperature while C_f^0 has no temperature dependence. Empirical modifications to CKDv0, based on various atmospheric and laboratory observations, have resulted in subsequent CKD versions, the latest of which is CKDv2.2. Although other spectral regions have undergone significant changes from CKDv0 to CKDv2.2, the 400 cm^{-1} to 600 cm^{-1} region has not. Until now, improvements and/or validation of the continuum models in the 400 cm^{-1} to 600 cm^{-1} region have been limited by a lack of observations; the work presented here contributes by providing the first observations of C_f^0 in this region since Burch’s original laboratory measurements. Collected at lower temperatures, these measurements may also provide information about the temperature dependence.

Observed and Calculated Radiances and Continuum Measurements

Line-by-line calculations of downwelling radiances were compared to observations for four selected clear-sky periods in October 1997. Steps taken to derive continuum coefficients from the observations are straightforward and

outlined here. For each case, clear-sky time periods were determined using a combination of observations that include 1) the AERI-ER spectra and their behavior for clear conditions, 2) time series of AERI-ER window channel radiances, 3) radiosondes, and 4) cloud radar. Individual AERI-ER spectra within these periods were averaged to produce mean spectra, along with uncertainties. Using profiles from Vaisala RS-80 radiosondes as input to Line-by-Line Radiative Transfer Model (LBLRTM), downwelling radiances were computed and convolved with the AERI-ER instrument function. Then, in deriving continuum values from the spectra, the calculations were repeated, but with the air-broadened continuum coefficients adjusted to produce agreement with the observations. No temperature dependence in C_f^0 was introduced and C_s^0 was not adjusted. This approach was followed independently for the four case studies and for each microwindow between 380 cm^{-1} and 596 cm^{-1} , yielding four sets of adjusted coefficients. The mean and the uncertainty in the mean of these values are plotted in Figure 2 as the solid curve with error bars. The error bars on the AERI-ER values therefore do not represent systematic errors, which might be present in all four cases. Also shown in Figure 2 are the room temperature laboratory measurements of Burch et al. and CKD model versions 0 and 2.2. Forty measurements of C_f^0 were made in 25 microwindows from 381.6 cm^{-1} to 596.3 cm^{-1} , with random uncertainties in the mean of less than 5% for 405 cm^{-1} and higher. Values at lower wavenumbers have larger uncertainties (up to 36% at 381.6 cm^{-1}) due to the low transmission of these channels and decreased signal-to-noise ratio of the instrument.

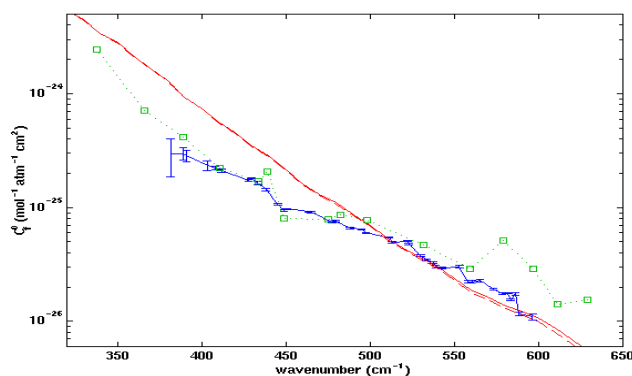


Figure 2. Air-broadened water vapor continuum coefficients, C_f^0 : CKD model versions 0 (solid red curve) and 2.2 (dashed red curve), laboratory measurements of Burch et al. (green squares) at 296 K, and determined from the SHEBA AERI-ER spectra in this work (solid blue curve with error-bars). (For a color version of this figure, please see http://www.arm.gov/docs/documents/technical/conf_9803/tobin-98.pdf).

For one of the case studies, Figure 3, shows observed, calculated radiances using the three sets of air-broadened continuum coefficients in Figure 2. The adjusted continuum coefficients clearly improve the agreement with the observed spectra. Comparisons for the other three case studies are nearly identical. This last point cannot be overstated; the fact that nearly identical error signatures and derived continuum coefficients are obtained for these four cases suggests that the results are not an artifact of cloud contamination or errors in the input water vapor profiles and that we are interpreting the radiance residuals in the correct manner.

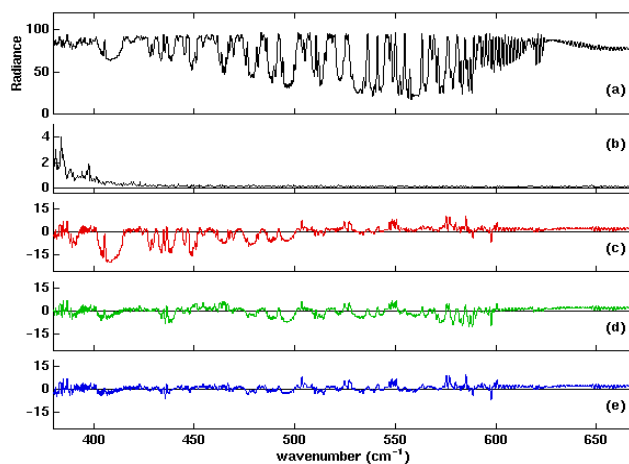


Figure 3. Observed and observed minus calculated downwelling radiances in the extended longwave region using various air-broadened water vapor continua: (a) mean observed radiance spectrum for the October 30 case; (b) uncertainty in the mean observed radiances (one standard deviation divided by the square root of the number of observations); (c) observed - calculated radiances using CKDv2.2 C_f^0 ; (d) same as (c) but using a linear interpolation through Burch's measured C_f^0 values; (e) same as (c) but using C_f^0 values determined from the four case studies presented in this work. (For a color version of this figure, please see http://www.arm.gov/docs/documents/technical/conf_9803/tobin-98.pdf).

From 400 cm^{-1} to 550 cm^{-1} , good agreement is found with Burch's 296 K laboratory measurements. The coefficients of this work were derived from spectra sensitive to a range of temperatures from roughly $\sim 230\text{ K}$ to 260 K , therefore providing evidence that C_f^0 has little or no temperature dependence near $25\text{ }\mu\text{m}$. This is a result that is also predicted by Ma and Tipping's (1992) calculations. Coefficients from this work, however, disagree with Burch's measurements from $\sim 560\text{ cm}^{-1}$ to 600 cm^{-1} , where Burch's

values suggest a localized increase in C_f^0 . In deriving the monomer lineshape associated with the initial CKDv0 model, equal weight was given to all of Burch's measurements, including the apparently erroneous values at higher wave numbers for this spectral region. These measurements suggest that CKDv2.2 (and CKDv0) C_f^0 is too large by a factor of ~ 3 at 400 cm^{-1} . The results of this will be incorporated into subsequent CKD models (Mlawer et al. 1998). A combination of these continuum measurements, others further into the rotational and ν_2 bands, accurate measurements of individual spectral line parameters, and a consistent lineshape formulation of the observed absorption, will provide the basis for accurate retrieval of middle and upper tropospheric water vapor from satellites and a quantitative description of the role these strong water bands play in climate. Lastly, the authors fully realize the sensitivity of these measurements to errors in the atmospheric water vapor profiles and the selection of clear-sky cases. Further refinements will be made as additional data are obtained. Spectra at lower temperatures and water vapor amounts are particularly crucial for deriving an accurate parameterization.

References

- Burch, D. E., and D. A. Gryvnak, 1979: Method of calculating H_2O transmission between 333 and 633 cm^{-1} . Tech. Rep. AFGL-TR-79-0054, Air Force Geophysics Lab., Hanscom AFB, Massachusetts.
- Clough, S. A., F. X. Kneizys, R. Davies, R. Gamache, and R. Tipping, 1980: Theoretical line shape for H_2O vapor; application to the continuum. In *Atmospheric Water Vapor*, edited by A. Deepak, T. D. Wilkerson, and L. H. Ruhnke, pp. 25-46, Academic Press.
- Clough, S. A., M. J. Iacono, and J.-L. Moncet, 1992: Line-by-line calculations of atmospheric fluxes and cooling rates: Application to water vapor. *J. Geophys. Res.*, **97**, 15,761-15,785.
- Ellingson, R. G., and W. J. Wiscombe, 1996: The spectral radiance experiment (SPECTRE): Project description and sample results. *Bull. Amer. Meteor. Soc.*, **77**, 1967-1985.
- Ma, Q., and R. H. Tipping, 1992: A far wing line shape theory and its application to the foreign-broadened water continuum absorption. III. *J. Chem. Phys.*, **97**, 818-828.
- Mlawer, E. J., S. A. Clough, P. D. Brown, and D. C. Tobin, 1998: A new formulation for the water vapor continuum. This proceedings.
- Sinha, A., and J. E. Harries, 1995: Water vapour greenhouse trapping: The role of far infrared absorption. *Geophys. Res. Lett.*, **22**, 2147-2150.
- Stamnes, K., R. G. Ellingson, J. A. Curry, J. E. Walsh, and B. D. Zak, 1998: Review of science issues, deployment strategy and status for the ARM North Slope of Alaska/Adjacent Arctic Ocean (NSA/AAO) Climate Research Site. *J. Climate*, in press.